

Roles of Cationic and Elemental Calcium in the Electro-Reduction of Solid Metal Oxides in Molten Calcium Chloride

Guohong Qiu^a, Kai Jiang^a, Meng Ma^a, Dihua Wang^a, Xianbo Jin^{a,b}, and George Z. Chen^{a,b}

^a College of Chemistry and Molecular Sciences, Wuhan University, Wuhan, 430072, P. R. China

^b School of Chemical, Environmental and Mining Engineering, University of Nottingham, Nottingham, NG7 2RD, UK

Reprint requests to G. Z. C.; E-mail: george.chen@nottingham.ac.uk

Z. Naturforsch. **62a**, 292–302 (2007); received March 3, 2007

Presented at the EUCHEM Conference on Molten Salts and Ionic Liquids, Hammamet, Tunisia, September 16–22, 2006.

Previous work, mainly from this research group, is re-visited on electrochemical reduction of solid metal oxides, in the form of compacted powder, in molten CaCl₂, aiming at further understanding of the roles of cationic and elemental calcium. The discussion focuses on six aspects: 1.) debate on two mechanisms proposed in the literature, i. e. electro-metallothermic reduction and electro-reduction (or electro-deoxidation), for the electrolytic removal of oxygen from solid metals or metal oxides in molten CaCl₂; 2.) novel metallic cavity working electrodes for electrochemical investigations of compacted metal oxide powders in high temperature molten salts assisted by a quartz sealed Ag/AgCl reference electrode (650 °C–950 °C); 3.) influence of elemental calcium on the background current observed during electrolysis of solid metal oxides in molten CaCl₂; 4.) electrochemical insertion/inclusion of cationic calcium into solid metal oxides; 5.) typical features of cyclic voltammetry and chronoamperometry (potentiostatic electrolysis) of metal oxide powders in molten CaCl₂; and 6.) some kinetic considerations on the electrolytic removal of oxygen.

Key words: Electro-Reduction; Calciothermic Reduction; Reactive Metal Oxides; Molten Calcium Chloride; Cyclic Voltammetry; Metallic Cavity Electrode.

1. Introduction

In the early 1960's, cathodic refining of liquid copper in molten BaCl₂ was first attempted in Cambridge [1]. In the experiments, the electrolytic cell consisted of a carbon anode and a liquid copper cathode, and the operation was in the constant current mode. The cell voltage varied with the electrolysis time in two stages. For example, at 0.31 A/cm², the voltage first increased gradually from 2.9 V to 3.6 V and then jumped suddenly to a plateau at 4.1 V. By product analysis Faradayic amounts of barium in samples collected from the second stage were detected, but not from the first stage. In both stages refining was achieved. About three decades later a similar procedure was applied in molten CaCl₂ for refining oxygenated solid titanium under a constant cell voltage control of about 3.0 V [2]. In both cases it was proposed that elemental barium or calcium was first formed at the cathode. The alkaline-earth metal consequently reacted with the oxygen atom (and other non-metallic impurities in the case of liq-

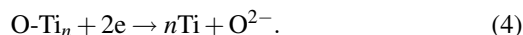
uid copper) in the metal to be refined, to form BaO or CaO [1, 2]. In the following text, for convenience of discussion, these proposed cathodic reactions are called *electro-metallothermic reduction* and summarized below using titanium and calcium as an example:



where O-Ti_n represents oxygen dissolved in solid titanium. Obviously, these reactions are thermodynamically equivalent to the reaction



The difference is that reaction (3) shows the *thermodynamic absence* of Ca and may occur at a less negative potential than reaction (1). Further, if CaO is completely dissociated into the Ca²⁺ and O²⁻ ions in the molten salt, reaction (3) can be simplified:



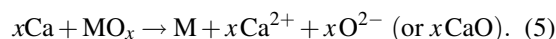
With emphasis on no involvement of elemental calcium, reactions (3) and (4) are termed as *electro-deoxidation* or *oxygen ionization* [3–7].

In the case of Cu refining, the two mechanisms can be differentiated by the detection of Ca or Ba, which dissolves readily in molten Cu to form the respective alloys [8]. As mentioned above and also shown by a re-investigation of the process in the constant voltage mode, oxygen removal from liquid Cu can be achieved solely via the oxygen ionisation mechanism [4]. Ti does not alloy with Ca or Ba, but deriving the mechanism is still experimentally possible if the activity of Ca in the molten salt can be correlated to the cathode potential and current. To obtain such a correlation is however challenging in a two-electrode cell, as was used in the experiments of [1] and [2], because the cathode potential and hence the Ca activity would vary with the cell current and/or the anode reaction(s). Therefore it is crucial to use a three-electrode cell in which the cathode potential is controlled or monitored against a reference electrode. Using a pseudo-reference electrode (e. g. a metal wire immersed in the same molten salt), preliminary results from a few cyclic voltammetric investigations of oxygenated liquid copper and titanium in molten BaCl₂ and CaCl₂ indeed revealed reduction current peaks at potentials noticeably more positive than that for Ca deposition [4, 6]. These observations agree with the oxygen ionisation mechanism.

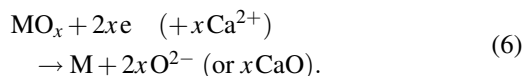
It was again in Cambridge in the late 1990's that electrolytic conversion of some solid metal oxides to the respective metals or alloys was achieved in molten salts, particularly TiO₂ in molten CaCl₂. These laboratory findings promise a completely new technology, namely the FFC Cambridge Process, for low-cost extraction of reactive metals and convenient synthesis of structural and functional alloys [3, 6, 7]. Although similar in the laboratory work to that of cathodic refining of metals, electrochemical reduction of solid metal oxides or simply *electro-deoxidation* or *electro-reduction* uses metal oxides as the cathode which are either insulators or poor conductors. Up till now, successful oxide-to-metal conversion has been achieved in pure CaCl₂ or BaCl₂ or their mixtures with alkali or alkaline-earth chlorides.

A debate then followed on the mechanisms of the cathodic oxide-to-metal conversion, particularly for TiO₂-to-Ti conversion. These two mechanisms are summarized below for a general form of metal oxides, MO_x [9–12]:

Electro-metallothermic reduction



Direct electro-reduction



Like the case of cathodic refining, differentiation between the two mechanisms is thermodynamically difficult, but kinetically possible. Particularly, for a porous oxide electrode made from compacted powder, the use of a three-electrode cell will allow correlation between the reduction current at controlled electrode (cathode) potentials and the Ca activity in the molten salt. This will in turn help to reveal which reaction is responsible for the current flow and hence for the oxide-to-metal conversion. In this paper, previously reported typical results from electro-reduction of some example oxide powders, such as NiO, Cr₂O₃, TiO₂ and Tb₂O₃, are discussed according to their cyclic voltammograms and/or chronoamperograms.

2. Novel Electrodes for Electro-Reduction under Potential Control

Satisfactory investigations by, for example, cyclic voltammetry and chronoamperometry require a reliable reference electrode for high temperature molten salts. It is also important to use a sufficiently small amount of oxide powder to construct the working electrode so that *iR* (voltage loss due to circuit and cell resistance) drop can be minimized without compromising the accuracy in measurement of the reduction current. In this group, a quartz sealed Ag/AgCl reference electrode, that is applicable at 650 °C ~ 950 °C [13], and two novel metallic cavity electrodes capable of loading sub-milligrams to milligrams of the oxide powder [14, 15] were constructed and exhibited very satisfactory performance in molten CaCl₂. Figure 1 illustrates these electrodes. While more details about fabrication of these electrodes and their application for electro-reduction can be found [13–15], main results are described here for the purpose of understanding the roles of elemental and cationic calcium in the electro-reduction of four typical metal oxides, namely NiO, Cr₂O₃, TiO₂ and Tb₂O₃.

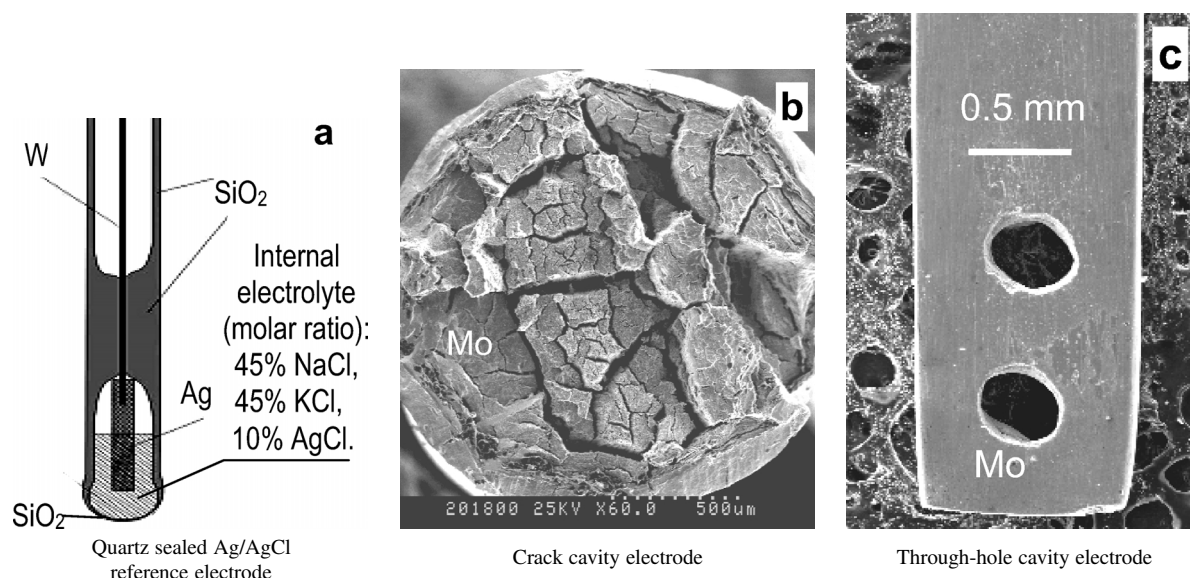


Fig. 1. Reference and working electrodes for cyclic voltammetry and chronoamperometry of metal oxide powders in high temperature molten salts. (a) Quartz sealed Ag/AgCl reference electrode [13]. (b) Cracked end-face of a Mo wire resulting from repetitive bending and fracturing at a pre-notched location [14]. (c) A 0.5 mm thick Mo foil with two laser-drilled through-holes [15]. The cracks or the through-holes in the electrodes were capable of securely holding oxide powders (sub-micron particle sizes, 0.1 ~ 1.0 mg) in molten salts.

3. Background Current in Molten CaCl_2

One of the practical issues in electrochemical investigations under controlled potential is the so-called background current. This is measurable by cyclic voltammetry or chronoamperometry. As an example, Fig. 2 shows a cyclic voltammogram (CV) recorded on a Mo foil working electrode in freshly prepared molten CaCl_2 . Similar CVs were reported previously in a three-electrode cell with a Ti metal pseudo-reference [6]. While the large reduction currents at potentials more negative than about -1.2 V are attributable to the deposition of Ca metal, the slowly increasing reduction currents at potentials between 0.9 V and -0.9 V represent the background currents. It was shown that, when the molten salt was more properly cleaned by, for example, pre-electrolysis, these background currents could be significantly reduced [15]. Therefore, impurities present in the molten salt were largely responsible.

When inspected for detail as shown by the inset of Fig. 2, it can be seen that the background currents are mostly cathodic in nature, which cannot be explained by the understanding of conventional reduction (positive current on forward potential scan) and re-oxidation (negative current on backward po-

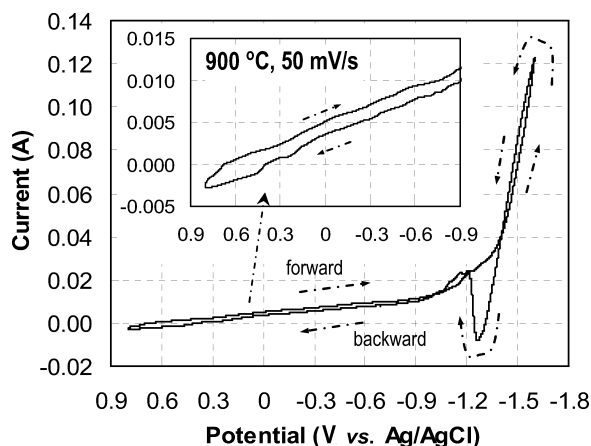


Fig. 2. Cyclic voltammogram of Mo foil in molten CaCl_2 .

tential scan) of active impurities. The sloped and linear variation of the background currents resembles what is expected from electronic conduction through the molten salt as described in detail in the literature via either direct electron transportation through molten salts (e.g. Na metal dissolved in molten NaCl) [16–18], or the inter-valence charge transfer (redox hopping) between multivalent transition metal ions (e.g. in mixed molten multivalent transition metal halides) [19–21].

It is worth noting that the currents on the forward and backward potential scans are parallel but different in magnitude. After further cleaning of the melt by, for example, a longer time of pre-electrolysis at ~ 2.6 V, the forward and backward background currents decreased in slope [15], but remained in separation and parallel. This behaviour is clearly capacitive in nature and may be linked to the electrode double layer which was likely non-ideal and hence could leak current under the conditions for recording the CV in Figure 2. The leaking element may be the electronic conduction through the melt, possibly resulting from 1.) inter-valence charge transfer between multivalent impurities, and 2.) the dissolved trace Ca whose activity is linked to the cathode potential. In fact, the double layer charging current was also observed in chronoamperometric measurements [15].

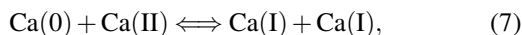
The authors' interest in the background currents is also due to the observed low current efficiency of electro-reduction of some solid metal oxides in molten CaCl_2 . In this group it was found that, when using a two-electrode cell, the current efficiency for electrolysis of pelletized TiO_2 powder of different origins in molten CaCl_2 was typically not greater than 20% [22, 23]. Similar results can also be found in or derived from literature reports by others [24, 25]. The current-time plots of electrolysis revealed a major contribution from the background current that flowed through the cell during the long and later electrolysis stage that was necessary to allow metallization to progress into the core of the oxide cathode (porous pellets) and also to achieve a low oxygen content in the obtained Ti metal. This background current is not the same as that shown in Fig. 2 and deserves more discussion.

The causes for the observed low current efficiency are complex. The problem is partly associated with the use of carbon as the anode material, leading to the formation of CO and CO_2 that can affect the electrolysis via 1.) electro-reduction at the cathode/electrolyte/gas three-phase interlines, and 2.) chemical reaction with CaO in the molten salt to form CO_3^{2-} which can then be converted to carbon via calciothermic and/or electrochemical reduction [24, 26]. The effect is two-fold: firstly, the electro-reduction of CO, CO_2 and CO_3^{2-} lowers the cathode efficiency; secondly, the resultant carbon may be in the form of carbonaceous debris and floats on the surface of the melt, forming a path for electronic conduction. (It should be mentioned that, besides the influence on the current efficiency,

the cathodic formation of carbon is more detrimental to the electro-reduction process by contamination of the product with carbon or carbide.) It should be pointed out that all the problems related with the carbon anode may be solved by using an inert anode when it becomes available. The application of a higher temperature (> 900 °C) can prevent the formation of CO_3^{2-} , and hence reduce the carbonaceous contamination [26]. Proper cell design and fabrication are also important against low current efficiency. According to the authors' experience, air leak to the high temperature reactor would lead to more serious carbonaceous contamination, and best effort must be applied to ensure a reliable gas-tight seal of the reactor. The thought that a positive inert gas pressure inside the reactor could prevent air from entering the reactor will undoubtedly lead to a unsatisfactory outcome in electro-reduction experiments.

In fact, even with a carbon anode, high current efficiency ($> 70\%$) has been achieved in electrolysis of, for example, Cr_2O_3 [26, 27], SiO_2 [28], and Ta_2O_5 [29]. In these cases, a lower cell voltage (< 2.8 V) and a shorter time (≤ 6 h, 2 g pellet) were sufficient to achieve low oxygen content in the products. However, for electrolysis of TiO_2 and Tb_2O_3 , for example, the cell voltage needs to be at or higher than 3.0 V. Taking the inevitable iR drop into consideration, it can be certain that electro-reduction of the oxide will dominate in the early stage of electrolysis when the current is high. Typically, for electrolysis of a 2 g pellet of compacted oxide powder, the initial current was greater than 2 A. The cell resistance, mainly from molten salt, was about 0.5 Ω . Thus, the iR drop was about 1 V, which means less than 2 V remained from the applied 3 V to drive the cathode and anode reactions. However, coming to the later stage of the electrolysis when the pellet was metallized on the surface and the current dropped below 1 A, the available cell voltage would become higher than that for decomposing CaO (~ 2.6 V). Consequently, with the anode reaction being the discharge of either the O^{2-} ion or CaO, elemental Ca may form at the cathode and dissolve in the molten salt. While the electro-decomposition of CaO itself reduces the current efficiency, the voltage-dependent but time-independent electrolysis current (background) suggests a more detrimental effect related with electronic conduction. Elemental Ca can dissolve slightly in molten CaCl_2 (~ 4 mol% at 900 °C) [9, 10] and likely contributes to the electron transportation through

the molten salt [16–18]. On the other hand, during electrolysis, the dissolved elemental Ca will inevitably transport to and be re-oxidized to the Ca^{2+} ion at the anode. This means that at the later stage of electrolysis, the concentration of elemental Ca would be lower than its solubility. Thus, an additional or alternative electron conduction path may be present as follows [22]:



The front-subscripts A and B in reactions (8) and (9) denote the relative positions of the species in the melt. The probability for reaction (9) to occur may be small because it requires simultaneous transfer of two electrons. Once such electron conduction paths are established in the melt, all the Ca(0) and Ca(I) species formed at the cathode will be balanced by their consumption/oxidation at the anode. In other words, there will not be any “net” increase of Ca(0) or Ca(I) on the cathode and in the melt. It also means that only a small amount of Ca(I) or (0) is needed in the molten salt to maintain a large electronic current. Further investigation is ongoing to search for evidence supporting this redox hopping process which resembles the inter-valence charge transfer mechanism.

4. Electrochemical Insertion/Inclusion of Cationic Calcium

In the electrolysis of solid TiO_2 (and some others such as Nb_2O_5 [30, 31]) in molten CaCl_2 , another main problem contributing indirectly to the low current efficiency is the electrochemical or chemical formation of various perovskite phases ($\text{Ca}_\delta\text{TiO}_x$, $\delta \leq 1$, $x \leq 3$) as the intermediate products [3, 22, 24]. These perovskite phases are larger in volume than the respective TiO_y ($y \leq 2$) phases because of the insertion or inclusion of Ca^{2+} ions. ($\rho_{\text{TiO}_2} = 4.23 \text{ g/cm}^3$, $\rho_{\text{Ti}_2\text{O}_3} = 4.49 \text{ g/cm}^3$, $\rho_{\text{CaTiO}_3} = 4.00 \text{ g/cm}^3$.) The consequent expansion of the solid phase reduces the number and sizes of pores in the cathode that are needed for the transport of O^{2-} ions. The $\text{Ca}_\delta\text{TiO}_x$ phases are also thermodynamically more stable than the TiO_y phases and require more negative potential to reduce. Both effects account partly for the low speed or long time electro-reduction of TiO_2 , and the low current efficiency in the presence of the electronic conduction [23].

The stoichiometry of two particular forms of the $\text{Ca}_\delta\text{TiO}_x$ phases has been recognized by XRD analyses to be CaTiO_3 (calcium titanate) to CaTi_2O_4 (calcium titanite) [25, 32]. Particularly, the chemical reaction between TiO_2 and CaO is thermodynamically favoured and was proposed to be responsible for the formation of CaTiO_3 [32]. Composition deviations from the two stoichiometries were also commonly observed in this group during elemental analysis [23]. Particularly, EDX analysis on individual crystallites revealed the Ca/Ti atomic ratio to be often much smaller than 1. Such stoichiometric differences can account for an electrochemically driven direct interaction between the Ca^{2+} ions and the TiO_y phases, and evidence from cyclic voltammetry was reported [6, 23]. The relevant electrode reaction is similar in form to that of the electrochemical intercalation of Li^+ into the Li_xCoO_2 phase. However, an initial change in structure is necessary to accommodate and transport the Ca^{2+} ions.

In this group it was observed that, when the molten CaCl_2 contained Mg^{2+} impurities ($\text{MgCl}_2 < 0.3 \text{ wt}\%$), both Mg(II) and Ca(II) were observed in the intermediate products. Using the metallic cavity electrode (Fig. 1c), cyclic voltammetry of TiO_2 powder revealed three main reduction current peaks before that for Ca deposition, as shown in Figure 3a. The two peaks at less negative potentials, C1 and C2, are associated with the chemical/electrochemical formation of the perovskite phases, and peak C3 is due to the reduction leading to metallic Ti [23, 32]. (Ca deposition current occurred at potentials more negative than the cathodic limit of the CVs in Figure 3.) These attributions have been confirmed by potentiostatic reduction of TiO_2 powder at different potentials around these three peaks. The products obtained after electrolysis for 1000 s are compared in Table 1 for composition and Fig. 4 for morphology. It can be seen that the Mg(II)-containing phases were more likely to form than the Ca(II) phases, implying that the smaller Mg^{2+} ion is more interactive with the TiO_y phases.

The correlations of the currents and potentials of the reduction peaks with the potential scan rate show typical features of irreversible electron transfer processes confined at the electrode [33]. Results from the analysis of peaks C2 and C3 are presented in Figs. 3b and 3c. These voltammetric features were also observed on other metal oxides [15], and are strong evidence for direct electron transfer between the current collector and the oxide. This agrees with the direct electro-reduction mechanism, but cannot be explained by the

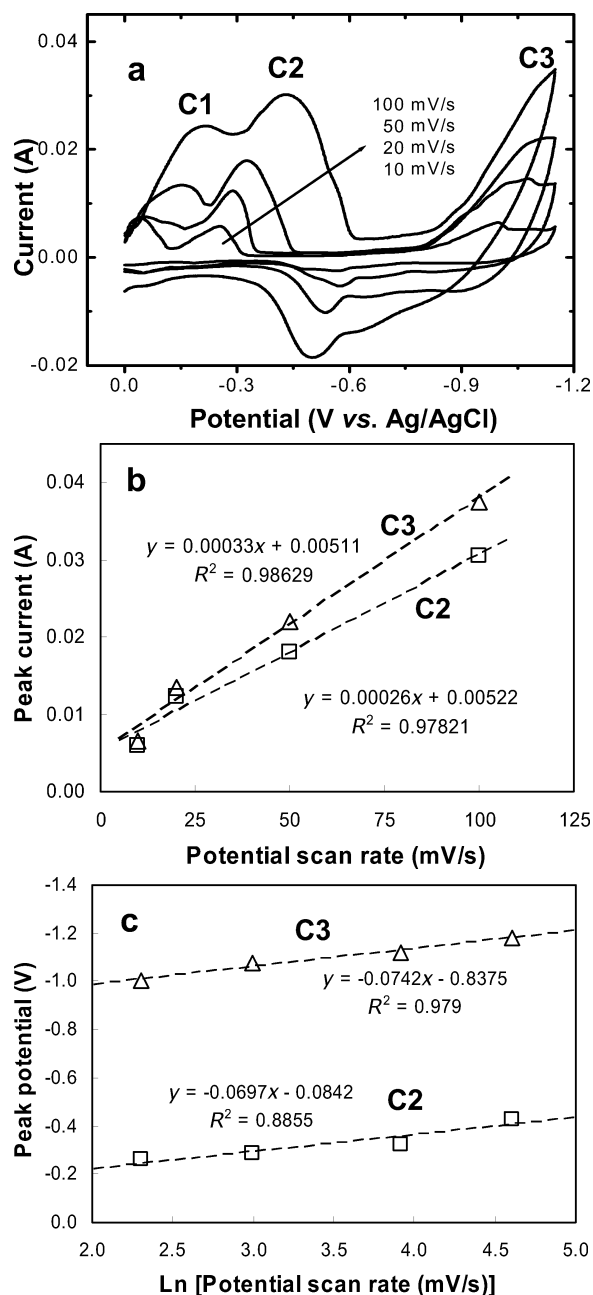


Fig. 3. (a) Cyclic voltammograms of a metallic cavity electrode (through-hole, Mo foil) with TiO_2 powder in molten CaCl_2 (+ MgCl_2 , ≤ 0.3 wt%) at 900°C and indicated potential scan rates. Each CV was recorded using a new electrode. (b, c) Correlations between (b) the peak current and potential scan rate and (c) the peak potential and logarithm of potential scan rate for peaks C2 and C3 of (a).

electro-metallothermic reduction mechanism. It is acknowledged that the early understanding of the electro-

Table 1. EDX analysis (at%) over the images shown in Figure 4.

Potential	O	Ca	Mg	Ti
-0.03 V	61.20	0.77	5.74	32.29
-0.25 V	59.31	n.d.	11.90	28.79
-0.45 V	59.90	0.41	10.56	29.13
-0.95 V	33.13	n.d.	n.d.	66.87
-1.15 V	20.76	n.d.	n.d.	79.24

n. d., not detected.

reduction mechanism did not include the intermediate steps involving interactions between the cationic calcium and the oxide. However, this process is not completely new, as discussed below.

The size effect between Ca^{2+} and Mg^{2+} ions is a convincing demonstration of the direct electrochemically driven interaction between the alkaline-earth cation and TiO_2 . Indeed, when TiO_2 electrolysis was carried out in molten LiCl , in which the Li^+ ion is even smaller, formation of stoichiometric compounds, LiTi_2O_4 and LiTiO_2 , was confirmed by X-ray and electron diffraction analyses and elemental analysis [14]. This process, although much faster because of the higher temperatures of the molten salt, is obviously the same as the well known electrochemical intercalation of Li^+ ions into the Li_xCoO_2 phase in the common lithium ion batteries. Of course, changes in structure and conductivity from TiO_2 to Li_xTiO_2 are necessary, and the results from cyclic voltammetry suggest the changes to be fairly fast in molten LiCl at 750°C [14]. In comparison, the larger Ca^{2+} and Mg^{2+} ions will find it to be more difficult to follow the same intercalation path of Li^+ ions, but may still be able to undergo a relatively shallow “intercalation” process.

It is worth mentioning that, with proper cathode designs and construction, both solid UO_2 and Ta_2O_5 have been electro-reduced to the respective metals in molten LiCl [34, 35]. In this group, attempts to reduce TiO_2 to Ti metal in molten LiCl were not successful. This was likely due to LiTiO_2 being thermodynamically more stable than LiCl .

In situ formation of the calcium-containing solid phases affects the electro-reduction of a number of oxides in molten CaCl_2 . It can be mostly avoided, at least for electro-reduction of TiO_2 , by ex situ “perovskitization”, a process to convert TiO_2 to perovskite by reaction with CaO at elevated temperatures [23]. In the preliminary test it was found that the electrolysis of porous CaTiO_3 was much shorter in time, leading to almost a double increase in current efficiency without compromising the product quality.

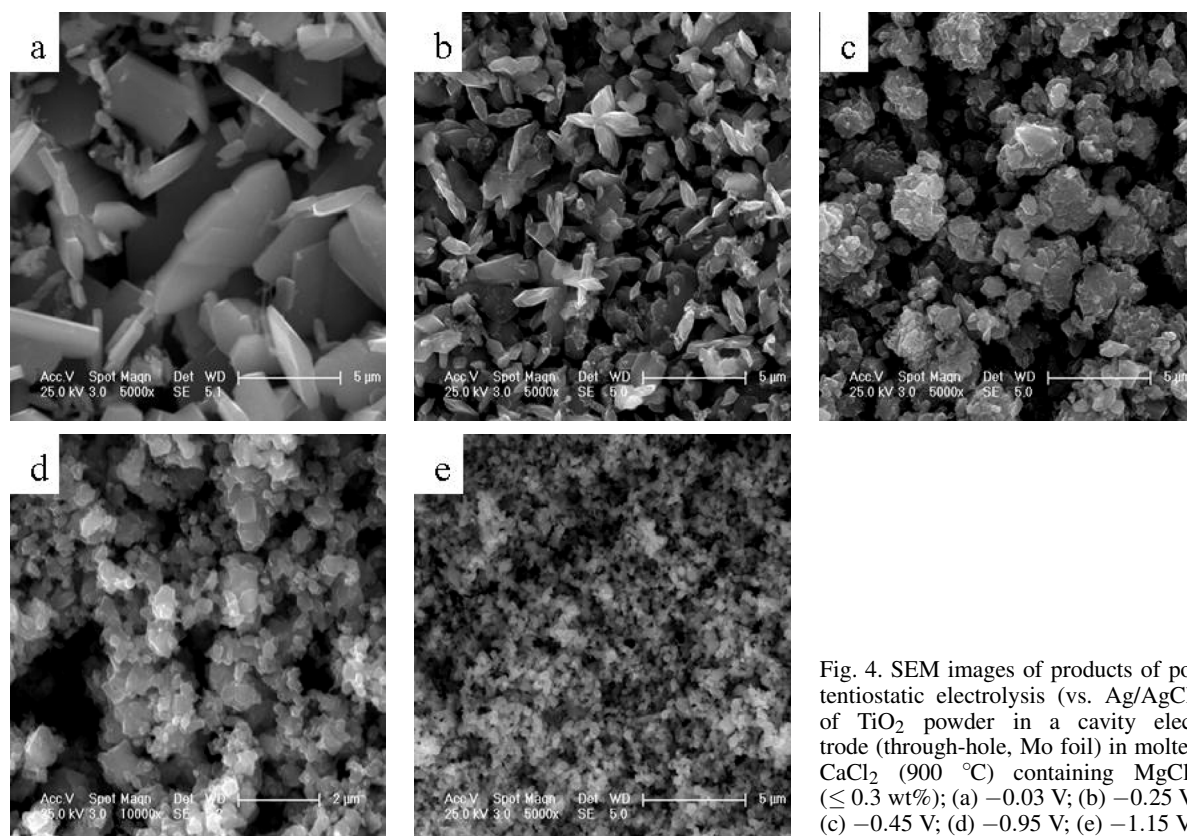


Fig. 4. SEM images of products of potentiostatic electrolysis (vs. Ag/AgCl) of TiO_2 powder in a cavity electrode (through-hole, Mo foil) in molten CaCl_2 ($900\text{ }^\circ\text{C}$) containing MgCl_2 ($\leq 0.3\text{ wt}\%$); (a) -0.03 V ; (b) -0.25 V ; (c) -0.45 V ; (d) -0.95 V ; (e) -1.15 V .

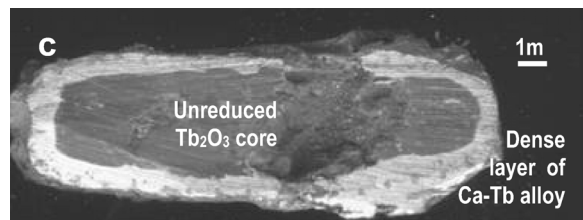
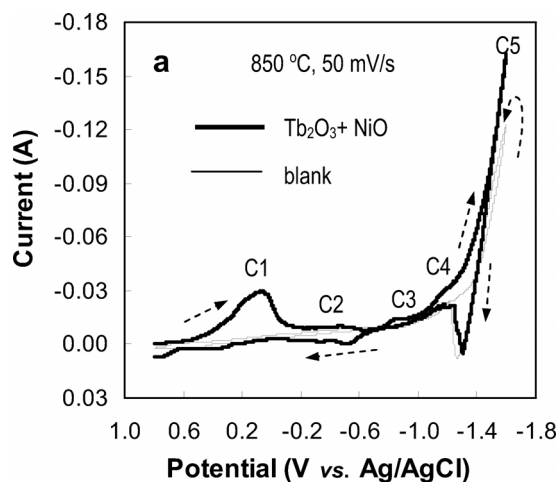
5. Cyclic Voltammetry and Chronoamperometry of Electro-Reduction of Metal Oxides

As discussed in the Introduction, when the oxide to be reduced in molten CaCl_2 is made into a cathode, it is difficult to thermodynamically differentiate reactions (1) and (5) from reaction (6), but the latter implies the formation of elemental calcium to be not necessary. However, it may be kinetically possible by investigations of the correlation between the cathode current and the cathode potential which is the determining factor of Ca activity in the molten salt [11]. Such an investigation cannot be reliably performed in a two-electrode cell but requires strict control of the electrode potential using a three-electrode cell with a reference electrode. Cyclic voltammetry and chronoamperometry (potentiostatic electrolysis) are the two reliable techniques, taking advantage of the three-electrode cell.

Using the electrodes shown in Fig. 1, cyclic voltammetry and chronoamperometry of a good number of metal oxides and oxide mixtures have been carried out

in molten salts in this group. Details of these investigations are presented above for TiO_2 and are also available in the literature [13–15, 23, 36, 37]. Here, some main findings are presented below.

1.) On all recorded cyclic voltammograms, the reduction current forms single or multiple peaks which are all electrochemically irreversible. In all cases, the peak current varies linearly with the potential scan rate, similar to what is shown in Figure 3b. This is a typical feature of a charge transfer process confined at the electrode, which agrees with the oxide powder being present in the electrode's cavity. The current onset potential is fairly independent of the potential scan rate and follows the same order as the oxide's thermodynamic stability with reference to that of CaO. Typically, for the oxide powders investigated by the metallic cavity electrode in this group the order is $\text{CaO} \sim \text{Tb}_2\text{O}_3 < \text{TiO}_2 < \text{Cr}_2\text{O}_3 < \text{Fe}_2\text{O}_3 < \text{NiO}$ (becoming less negative). However, the potentials at which the reduction currents are observed, including that of the current peak, shift negatively and linearly with the logarithm of the scan rate, as predicted for



an irreversible surface-confined electron transfer process [33].

2.) The CVs of TiO_2 powder show at least three main reduction peaks, as shown in Fig. 3a, including those corresponding to the formation of the perovskite phases (peaks C1 and C2). However, NiO , Fe_2O_3 and Cr_2O_3 exhibited only a minor CV feature of slowly increasing current over a wide potential range (200 ~ 400 mV), before a main irreversible reduction peak at potentials that are still far more positive than that for Ca deposition. In these three oxides, no calcium-containing oxide phases were observed in the cavity electrode, although Mg^{2+} -containing phases were observed at reducing Cr_2O_3 [15]. Because Cr_2O_3 was previously reported to form various calcium chromate/chromite phases [26,27], it is then likely that the small volume of the cavity electrode allowed fast dispersing of the O^{2-} ions into the molten salt and hence prevented the chemical reaction between CaO and Cr_2O_3 or its partially reduced forms.

3.) The reduction of Tb_2O_3 is found to occur in a potential range extended into the region where Ca^{2+} reduction occurs, as shown by the CVs in Fig. 5a recorded using the metallic cavity electrode [38]. Again, no calcium-containing oxide phases are observed. The speed of Tb_2O_3 reduction to Tb metal is

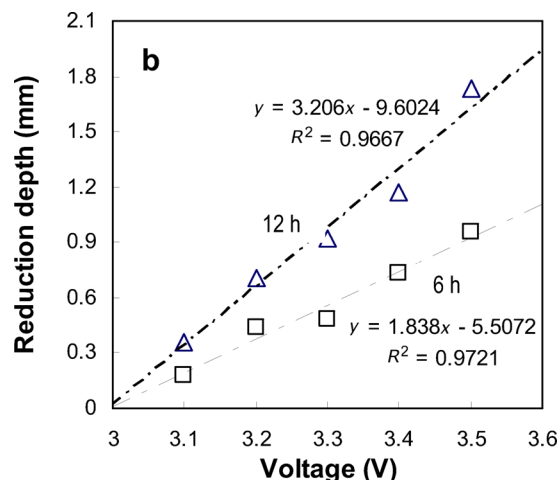


Fig. 5. (a) Cyclic voltammograms of a Mo cavity electrode with and without mixed powders of $\text{Tb}_2\text{O}_3 + \text{NiO}$ (molar ratio 1 : 10) in molten CaCl_2 . (b) Correlation between the reduction depth and the applied cell voltage in constant voltage electrolysis of a Tb_2O_3 pellet for 6 h (triangle marks) and 12 h (square marks) in molten CaCl_2 at 850 °C. (c) Image of the cross section of a Tb_2O_3 pellet electrolyzed at 4.2 V for 6 h [36, 37].

found to increase continuously with increasing the cell voltage well beyond that for CaO and CaCl_2 decomposition (respectively 2.686 V and 3.245 V at 850 °C), until the cathode is completely enclosed by a dense layer of Ca-Tb alloy as shown in Figure 5b. According to the electro-metallothermic reduction mechanism, the reduction speed will no longer increase after the Ca activity reaches unity, i. e. the formation of a distinct Ca phase that can be represented by a single drop of liquid Ca metal at the cathode, disregarding the cathode potential. However, the almost linear increase of the reduction speed with the cell voltage increasing up to about 3.6 V in Fig. 5b demonstrates strongly that the reduction of Tb_2O_3 is controlled by the cathode potential, instead of the Ca activity which should have reached unity at a much lower voltage.

4.) Potentiostatic electrolysis or chronoamperometry of metal oxide powders can very conveniently and quickly be performed using the metallic cavity electrode. Selection of potentials for the electrolysis is according to the CV, so that the reaction at each of the feature potentials on the CV can be identified by for example EDX. Typical results are presented in Fig. 6 for electro-reduction of Cr_2O_3 [15]. In this type of experiments, the mass of the oxide powder contained in the cavity can be weighed using an accurate balance to the

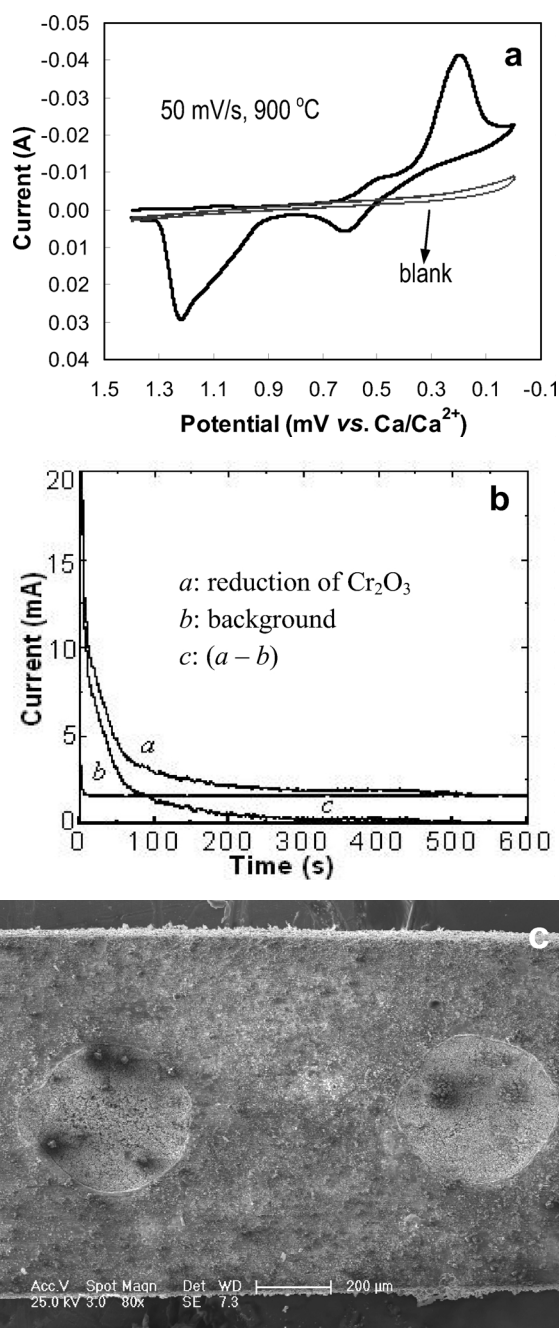


Fig. 6. (a) Cyclic voltammograms of a metallic cavity electrode with and without the Cr₂O₃ powder. Note: The zero potential is given vs. Ca/Ca²⁺ (≈ -1.2 V vs. Ag/AgCl). (b) Current-time plots of potentiostatic electrolysis of a metallic cavity electrode at 0.3 V (vs. Ca/Ca²⁺) and 900 °C in molten CaCl₂ [15]. (c) SEM image of the metallic cavity electrode taken after potentiostatic reduction.

level of sub-milligrams. This mass can then be correlated with the charge passed according to the Coulombic relationship as predicted from an assumed electrode reaction at the selected potential from the CV. The net charge passed in Fig. 6b is found to agree very well with the calculated value from the mass for the reduction of Cr₂O₃ to Cr metal. The Coulombic efficiency (theoretical charge/measured charge) was as high as 98.5%. The material in the cavity after electrolysis can be investigated by SEM (Fig. 6c) and EDX, which is particularly useful for determining the nature of product at any potential and electrolysis time [15]. Note that plot *b* in Fig. 6b was recorded in the absence of any oxide and shows clearly a current jump at the very beginning of the electrolysis, and later a stable background current. The two chronoamperometric features correspond, respectively, to an electrode double layer charging and, very likely, electronic conduction through the molten salt as discussed before.

6. Electro-Reduction vs. Electro-Metallothermic Reduction

According to the kinetics, the overall rate of reactions (1) and (5) is determined by the slower one of the two. If reaction (5) is slower, reaction (1) would be at equilibrium and the Ca activity should follow the cathode potential. Therefore, at certain potentials, there could be excess Ca in the molten salt when Ca supply from reaction (1) exceeds the need of reaction (5), and the current flow at the oxide cathode should follow the same path as if a bare inert metal cathode was used. The corresponding CV will be the same as that shown in Fig. 2, which however contradicts to the CVs of all the tested metal oxides recorded using the metallic cavity electrodes [15, 23] and other types of electrode [6, 26, 29, 32].

If reaction (1) is slower, reaction (5) will continuously remove the elemental Ca from reaction (1), leading to a Ca activity lower than what would be determined by the cathode potential. Consequently, the reduction current can flow high even at potentials more positive than that of reactions (1) alone. On the other hand, at a sufficiently high speed of oxide reduction, the Ca activity must also be high at the electrode. Because of its relatively high solubility, part of the Ca generated by reaction (1) can dissolve in and diffuse into the molten salt and hence is not consumed by reaction (5). Therefore, a lower Coulombic efficiency would have been inevitable at high reduction speed (or

high reduction current). On the contrary, upon subtraction of the background current measured in the absence of any oxide, very high Coulombic efficiency (98.5% for Cr_2O_3) was derived from potentiostatic (or chronoamperometric) reduction of, for example, NiO and Cr_2O_3 using the metallic cavity electrode at potentials where high reduction current was observed [15].

The above discussion on electro-metallothermic reduction is far from being exhaustive, but does demonstrate the difficulties of this old-fashioned understanding of pyro-metallurgical processes. On the other hand, when an oxide is reduced by Ca metal in molten CaCl_2 , the Ca plays the simple role of an electron donor. A current collector can do equally in molten CaCl_2 , and this possibility is completely ignored by the electro-metallothermic reduction mechanism. Another cause for the argument is likely due to the facts that metal oxides are usually insulators or poor electric conductors that are out of the question according to conventional knowledge of electrolysis, and that the understanding of electro-reduction at the metal/metal oxide/electrolyte three-phase interlines is also relatively new [12, 27, 28].

7. Summary

This paper reviews recent research findings in relation with the roles of cationic and elemental calcium in the processes of electro-reduction of solid metal oxides in molten CaCl_2 . It is shown that the electro-reduction process is dominated by direct electron transfer to the metal oxide, with very little, if any, contribution from elemental Ca. Even in the presence of a large amount

of cathodically formed elemental Ca, the reduction of Tb_2O_3 was retarded because of the formation of a dense layer of Ca-Tb alloy on the surface of the oxide cathode. A redox hopping process, which is similar to the inter-valence charge transfer process, is proposed to be present between elemental and cationic calcium, contributing at least partly to the electronic conduction through the molten salt. On the other hand, based on confirmed electrochemical intercalation of Li^+ into TiO_2 in molten LiCl , it is proposed that cationic Ca (i.e. Ca^{2+}) does affect the electro-reduction process via a step similar to electrochemical intercalation, but possibly in a very shallow manner, to form various perovskite phases in addition to the chemical reaction between CaO and the metal oxide. Finally, a discussion in terms of kinetics is given, aiming at distinguishing between direct electron transfer from the electrode to solid metal oxide (electro-reduction) and the electro-metallothermic reduction mechanism, which emphasises the electrochemical reduction of the Ca^{2+} ion to elemental Ca as the necessary first step followed by a calciothermic reduction of the metal oxide. The discussion is not exhaustive but has already revealed difficulties of verifying the electro-metallothermic reduction mechanism with experimental findings.

Acknowledgement

The Natural Science Foundation of China (Grant Nos. 20403012, 20125308, 20573081, 50374052) and The Royal Society (2005-06 China Fellowship of X. J. and G.Z. C.) are gratefully acknowledged for financial support. G. Q., K. J. and M. M. each made equal contribution to this work.

- [1] R. G. Ward and T. P. Hoar, *J. Inst. Met.* **90**, 6 (1961).
- [2] T. H. Okabe, M. Nakamura, T. Oishi, and K. Ono, *Met. Mater. Trans. B* **24**, 449 (1993).
- [3] D. J. Fray, T. W. Farthing, and Z. Chen, International Patent, PCT/GB99/01781, WO99/64638 (1999) (Priority UK filing: GB9812169, 5 June 1998).
- [4] G. Z. Chen and D. J. Fray, *J. Appl. Electrochem.* **31**, 155 (2001).
- [5] G. Z. Chen, D. J. Fray, and T. W. Farthing, *Met. Mater. Trans. B* **36**, 1041 (2001).
- [6] G. Z. Chen and D. J. Fray, *J. Electrochem. Soc.* **149**, E455 (2002).
- [7] G. Z. Chen, D. J. Fray, and T. W. Farthing, *Nature* **407**, 361 (2000).
- [8] H. Massalski (Ed.), *Binary Alloy Phase Diagrams*, ASM International, The Materials Information Society, Metals Park, Ohio, USA 1990, Ca-Cu, Vol. 1, p. 907, and Cu-Ba, Vol. 1, p. 573.
- [9] K. Ono and R. O. Suzuki, *JOM-J. Min. Met. Mater. Soc.* **54**, 59 (2002).
- [10] R. O. Suzuki, *J. Phys. Chem. Solids* **66**, 461 (2005).
- [11] D. J. Fray and G. Z. Chen, in: *Cost-Affordable Titanium* (Eds. F. H. Froes, M. A. Imam, and D. J. Fray), TMS, Warrendale 2004, pp. 9–17.
- [12] G. Z. Chen and D. J. Fray, *Light Met.*, 881 (2004).
- [13] P. Gao, X. B. Jin, D. H. Wang, X. H. Hu, and G. Z. Chen, *J. Electroanal. Chem.* **579**, 321 (2005).
- [14] K. Jiang, X. H. Hu, H. J. Sun, D. H. Wang, X. B. Jin, Y. Y. Ren, and G. Z. Chen, *Chem. Mater.* **16**, 4324 (2004).
- [15] G. H. Qiu, M. Ma, D. H. Wang, X. B. Jin, X. H. Hu, and G. Z. Chen, *J. Electrochem. Soc.* **152**, E328 (2005).

- [16] G.M. Haarberg, J. Thonstad, J.J. Egan, R. Oblakowski, and S. Pietrzyk, *Ber. Bunsenges. Phys. Chem.* **102**, 1314 (1998).
- [17] G.M. Haarberg, K.S. Osen, R.J. Heus, and J.J. Egan, *J. Electrochem. Soc.* **137**, 2777 (1990).
- [18] G.M. Haarberg, K.S. Osen, J.J. Egan, H. Heyer, and W. Freyland, *Ber. Bunsenges. Phys. Chem.* **92**, 139 (1988).
- [19] U. Stohr and W. Freyland, *Phys. Chem. Chem. Phys.* **1**, 4383 (1999).
- [20] S.Z. El Abedin, O. Terakado, F. Endres, D. Nattland, and W. Freyland, *Phys. Chem. Chem. Phys.* **4**, 5335 (2002).
- [21] W. Freyland, *Z. Phys. Chem.* **184**, 139 (1994).
- [22] M. Ma, D.H. Wang, W.G. Wang, X.H. Hu, X.B. Jin, and G.Z. Chen, *J. Alloys Compd.* **420**, 37 (2006).
- [23] K. Jiang, X.H. Hu, M. Ma, D.H. Wang, G.H. Qiu, X.B. Jin, and G.Z. Chen, *Angew. Chem. Int. Ed. Engl.* **45**, 428 (2006).
- [24] M.F. Liu, Z.C. Guo, and W.C. Lu, *Trans. Inst. Min. Metall. Sect. C – Miner. Process. Extr. Metall.* **114**, C87 (2005).
- [25] C. Schwandt and D.J. Fray, *Electrochim. Acta* **51**, 66 (2005).
- [26] E. Gordo, G.Z. Chen, and D.J. Fray, *Electrochim. Acta* **49**, 2195 (2004).
- [27] G.Z. Chen, E. Gordo, and D.J. Fray, *Met. Mater. Trans. B* **35**, 223 (2004).
- [28] W. Xiao, X.B. Jin, Y. Deng, D.H. Wang, X.H. Hu, and G.Z. Chen, *Chem. Phys. Chem.* **7**, 1750 (2006).
- [29] T. Wu, X.B. Jin, W. Xiao, X.H. Hu, D.H. Wang, and G.Z. Chen, *Chem. Mater.* **19**, 153 (2007).
- [30] X.Y. Yan and D.J. Fray, *J. Electrochem. Soc.* **152**, D12 (2005).
- [31] X.Y. Yan and D.J. Fray, *J. Electrochem. Soc.* **152**, E308 (2005).
- [32] K. Dring, R. Dashwood, and D. Inman, *J. Electrochem. Soc.* **152**, E104 (2005).
- [33] A.J. Bard and L.R. Faulkner, *Electrochemical Methods – Fundamentals and Applications*, 2nd ed., John Wiley & Sons, Inc, New York 2001.
- [34] Y. Sakamura, M. Kurata, and T. Inoue, *J. Electrochem. Soc.* **153**, D31 (2006).
- [35] C.-S. Seo, S.-M. Jeong, S.-B. Park, J.-Y. Jung, S.-W. Park, and S.H. Kim, *J. Chem. Eng. Jpn.* **39**, 77 (2006).
- [36] G.H. Qiu, D.H. Wang, X.B. Jin, and G.Z. Chen, *Electrochim. Acta* **51**, 5785 (2006).
- [37] G.H. Qiu, D.H. Wang, M. Ma, X.B. Jin, and G.Z. Chen, *J. Electroanal. Chem.* **589**, 139 (2006).
- [38] D.H. Wang, G.H. Qiu, X.B. Jin, X.H. Hu, and G.Z. Chen, *Angew. Chem. Int. Ed. Engl.* **45**, 2384 (2006).